WF (*15*) and to cell wall preparations of the Gram-negative eubacterium *E. coli* DH5α (Fig. 3, C and D) (*18*). No binding was detected for whole cells (*15*) or for cell wall preparations (Fig. 3, E and F) of strain 195.

The phylogenetic position of strain 195 was determined on the basis of its 16S ribosomal DNA sequence (Fig. 4). The PCE dechlorinator grouped within the eubacteria in all analyses but did not cluster within any of the known phylogenetic lines. Although the maximum likelihood analysis presented places strain 195 on a branch that includes cyanobacteria and planctomycetes, DNA distance analyses placed it closer to *Clostridium butyricum* and its relatives (*19*) but with little affiliation for other members of the Gram-positive branch. Thus, its relationship with the presently described eubacterial branches is unclear at this time. It is clearly distinct from other recent isolates that reduce PCE to *cis*-DCE (*9*), which are affiliated with the ε and γ branches of the Proteobacteria or with the Gram-positive sulfate-reducing bacteria. Because strain 195 does not appear to belong to any presently known genus or species, we suggest naming it *Dehalococcoides ethenogenes* strain 195, pending a more thorough taxonomic description.

In summary, we isolated an organism that is capable of respiratory reductive dechlorination of PCE completely to ETH with H_2 as an electron donor. Previous isolates reduce PCE only as far as *cis*-DCE. It is of interest that at many PCE-contaminated sites, dechlorination proceeds only as far as *cis*-DCE, whereas at other sites VC and ETH are produced (*3*). It is not clear whether incomplete dechlorination at a given site is due to suboptimal physiochemical conditions, deficiencies in electron donors or nutrients present, or a lack of appropriate organisms.

REFERENCES AND NOTES

1. P. H. Abelson, *Science* **250**, 73 (1990).
2. J. J. Westrick, J. W. Mello, R. F. Thomas, *J. Am. Water Works Assoc.* **76(5)**, 52 (1984).
3. R. E. Hinchee, A. Leeson, L. Semprini, Eds., *Bioremediation of Chlorinated Solvents* (Battelle, Columbus, OH, 1995).
4. D. L. Freedman and J. M. Gossett, *Appl. Environ. Microbiol.* **55**, 2144 (1989).
5. W. P. de Bruin, M. J. J. Kotterman, M. A. Posthumus, G. Schraa, A. J. B. Zehnder, *ibid.* **58**, 1996 (1992).
6. C. J. Gantzer and L. P. Wackett, *Environ. Sci. Technol.* **25**, 715 (1991).
7. B. D. Ensley, *Annu. Rev. Microbiol.* **45**, 283 (1991).
8. W. W. Mohn and J. M. Tiedje, *Microbiol. Rev.* **56**, 482 (1992).
9. C. Holliger, G. Schraa, A. J. M. Stams, A. J. B. Zehnder, *Appl. Environ. Microbiol.* **59**, 2991 (1993); H. Scholz-Muramatsu, A. Neumann, M. Messmer, E. Moore, G. Diekert, *Arch. Microbiol.* **163**, 48 (1995); P. K. Sharma and P. L. McCarty, *Appl. Environ. Microbiol.* **62**, 761 (1996); J. Gerritse *et al.*, *Arch. Microbiol.* **165**, 132 (1996); L. R. Krumholz, R. Sharp, S. S. Fishbain, *Appl. Environ. Microbiol.* **62**, 4108 (1996).
10. T. D. DiStefano, J. M. Gossett, S. H. Zinder, *Appl. Environ. Microbiol.* **57**, 2287 (1991).
11. ———, *ibid.* **58**, 3622 (1992).
12. D. E. Fennell, M. A. Stover, S. H. Zinder, J. M. Gossett, in (*3*), pp. 9–16.
13. V. Tandoi, T. D. DiStefano, P. A. Bowser, J. M. Gossett, S. H. Zinder, *Environ. Sci. Technol.* **28**, 973 (1994).
14. X. Maymó-Gatell, V. Tandoi, J. M. Gossett, S. H. Zinder, *Appl. Environ. Microbiol.* **61**, 3928 (1995).
15. X. Maymó-Gatell, Y.-t. Chien, J. M. Gossett, S. H. Zinder, data not shown.
16. J. J. Bozzola and L. D. Russell, *Electron Microscopy: Principles and Techniques for Biologists* (Jones and Bartlett, Boston, MA, 1992), pp. 16–37.
17. O. Kandler, *Syst. Appl. Microbiol.* **16**, 501 (1994).
18. R. K. Sizemore, J. J. Caldwell, A. S. Kendrick, *Appl. Environ. Microbiol.* **56**, 2245 (1990).
19. M. D. Collins *et al.*, *Int. J. Syst. Bacteriol.* **44**, 812 (1994).
20. G. D. Sprott, S. F. Koval, C. A. Schnaitman, in *Methods for General and Molecular Microbiology*, P. Gerhardt, Ed. (American Society for Microbiology, Washington, DC, 1994), pp. 72–103.
21. B. L. Maidak *et al.*, *Nucleic Acids Res.* **22**, 3485 (1994).
22. D. C. Goodwin and S. B. Lee, *Biotechniques* **15**, 438 (1993).
23. J. L. Johnson, in *Methods for General and Molecular Microbiology*, P. Gerhardt, Ed. (American Society for Microbiology, Washington, DC, 1994), pp. 683–700.
24. J. Felsenstein, Phylogenetic inference program (PHYLIP) manual version 3.5c (University of Washington, Seattle, WA, 1993). http://evolution.genetics.washington.edu/phylip.html

25. Supported by the U.S. Air Force Armstrong Laboratory, Environmental Quality Directorate, Tyndall Air Force Base, FL; the Cornell Center for Advanced Technology in Biotechnology; and the "La Caixa" Foundation, Catalonia, Spain (X.M.-G.). We thank T. Anguish, S. McKay, and C. Bakermans for technical assistance; W. C. Ghiorse, B. Eglesham, and R. Garen for assistance in electron and fluorescence microscopy; and D. Fennell for providing culture material.

22 April 1996; accepted 14 April 1997

Membrane and Morphological Changes in Apoptotic Cells Regulated by Caspase-Mediated Activation of PAK2

Thomas Rudel* and Gary M. Bokoch†

Apoptosis of Jurkat T cells induced the caspase-mediated proteolytic cleavage of p21-activated kinase 2 (PAK2). Cleavage occurred between the amino-terminal regulatory domain and the carboxyl-terminal catalytic domain, which generated a constitutively active PAK2 fragment. Stable Jurkat cell lines that expressed a dominant-negative PAK mutant were resistant to the Fas-induced formation of apoptotic bodies, but had an enhanced externalization of phosphatidylserine at the cell surface. Thus, proteolytic activation of PAK2 represents a guanosine triphosphatase–independent mechanism of PAK regulation that allows PAK2 to regulate morphological changes that are seen in apoptotic cells.

Apoptosis, or regulated cell death, is a fundamental process in the development of multicellular organisms. Although it is initiated by many physiologic and pathologic stimuli, all apoptotic cells undergo a similar sequence of morphological and biochemical events (*1*). The cascade of ICE/CED-3 family cysteine proteases (termed caspases) (*2*) is a common and critical component of the cell death pathway (*3*, *4*). The identified targets for proteolytic cleavage by caspases are few, and the role of individual targets in mediating particular apoptotic events remains ill-defined.

p21-activated kinases (PAKs) are serine-threonine kinases whose activity is regulated by the small guanosine triphosphatases (GTPases) Rac and Cdc42 (*5*, *6*). PAKs regulate morphological and cytoskeletal changes in a variety of cell types (*7*, *8*), implicating PAKs as downstream mediators of the effects of Rac and Cdc42 on the actin cytoskeleton. Immunoblot analysis (*9*) reveals that Jurkat T cells predominantly express the 62-kD PAK2 isoform. An apparent decrease in the intensity of the 62-kD PAK2 band is observed after induction of Jurkat cell death by Fas receptor cross-linking (*10*). A 34-kD COOH-terminal PAK2 fragment (Fig. 1A) and a 28-kD NH_2-terminal PAK2 fragment (Fig. 1B) appeared after 1 hour, suggesting that PAK2 is cleaved into two defined fragments during Fas-induced apoptosis (*11*). In detailed time-course studies, PAK2 cleavage was detected as early as 30 min after stimulation by immunoglobulin M (IgM) antibody to Fas (anti-Fas) and the cleavage of PAK2 always correlated with the onset of apoptotic cell death. PAK2 cleavage was also observed when apoptosis was induced in Jurkat cells with C2 ceramide or in MCF-7 cells with tumor necrosis factor–α (TNF-α) (Fig. 1C), suggesting that this is a general phenomenon in apoptotic cells.

Department of Immunology, The Scripps Research Institute, 10550 North Torrey Pines Road, La Jolla, CA 92037, USA

*Present address: Max-Planck-Institut für Infektionsbiologie, Abt. Molekulare Biologie, Mobijoustrassse 2, D-10117 Berlin, Germany.

†To whom correspondence should be addressed.

Because the cleavage of PAK2 correlated with the onset of apoptosis, we reasoned that caspases might proteolytically cleave PAK2. Jurkat T cells were incubated with the caspase inhibitors YVAD-CMK (*12*) or DEVD-ald (*13*) before Fas receptor ligation, and PAK2 processing and apoptosis were monitored (Fig. 1D). Both DEVD-ald and YVAD-CMK peptides substantially inhibited cleavage of PAK2. In a broken cell apoptotic lysate (*14*), DEVD-ald totally blocked cleavage of a purified histidine-tagged PAK2 fusion protein (H6PAK2H6) (*15*) at concentrations as low as 0.1 μM, whereas YVAD-CMK was at least 100-fold less potent (*16*). As DEVD peptides are inhibitors of CPP32 (caspase 3)-like proteases (*13*), we compared the in vitro cleavage of H6PAK2H6 using lysates of Fas-activated Jurkat cells to cleavage by recombinant CPP32 (rCPP32) expressed as a glutathione-S-transferase (GST) fusion protein in *Escherichia coli* (*17*). rCPP32 cleaved H6PAK2H6 to a 34-kD COOH-terminal fragment (Fig. 2A) and a 28-kD NH_2-terminal fragment (*16*) of the same size as those produced by activated Jurkat lysates.

PAK2 contains several potential CPP32 cleavage sites (*18*), some of which are also present in PAK1. To determine if both PAK1 and PAK2 were caspase substrates, we treated purified PAK1H6 and PAK2H6 with lysates of Fas-induced Jurkat cells under identical conditions (*14*). PAK2 was processed to the 34-kD COOH-terminal cleavage product, whereas PAK1 was not cleaved (Fig. 2B). The CPP32 cleavage site in PAK2 was identified as the position adjacent to Asp^{212} by mutagenesis to asparagine (*19*). Thus, H6PAK2H6D212N was not proteolytically cleaved to the 34-kD COOH-terminal fragment by rCPP32 (Fig. 2C), nor in apoptotic cell lysates containing endogenous CPP32-like caspases. The predicted sizes of the PAK2 proteolytic fragments resulting from cleavage at Asp^{212} are consistent with what is observed (~34 and ~28 kD). We therefore conclude that CPP32 cleaves PAK2 after Asp^{212}. Although PAK1 also contains an aspartic acid residue at the homologous position as PAK2, this site is surrounded by a number of features (for example, continuous proline residues) that are likely to disrupt recognition by caspases. PAK3 lacks the relevant aspartate residues and thus the consensus caspase cleavage site.

PAKs consist of two major functional domains, an NH_2-terminal regulatory domain and the COOH-terminal catalytic domain (*5*, *7*). Because the 34-kD PAK2 cleavage product apparently contains the complete catalytic domain (*5*), the removal of the regulatory domain by cleavage of PAK2 during Fas-induced apoptosis might be sufficient to cause PAK2 kinase activation. By use of in-gel kinase assays (*20*), a p47*phox* peptide–dependent kinase activity (*21*) of 34 kD appeared

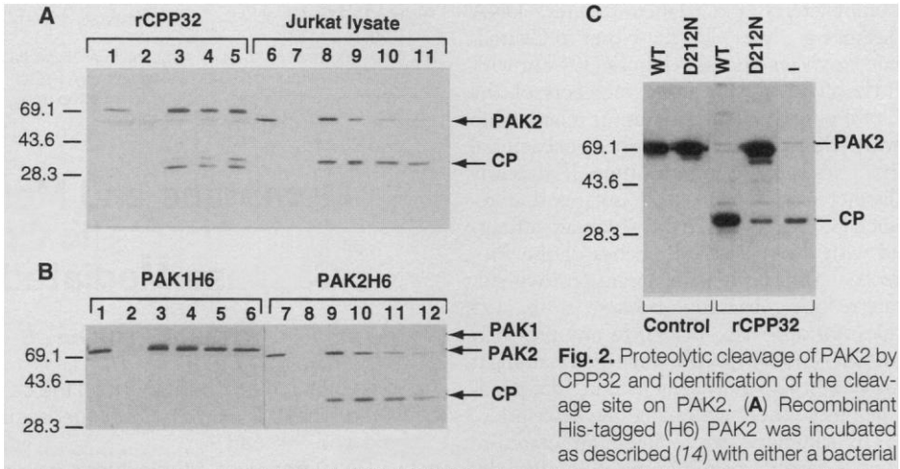

Fig. 2. Proteolytic cleavage of PAK2 by CPP32 and identification of the cleavage site on PAK2. (**A**) Recombinant His-tagged (H6) PAK2 was incubated as described (*14*) with either a bacterial lysate overexpressing recombinant CPP32 (rCPP32) or a cell lysate prepared from Fas-stimulated Jurkat cells undergoing apoptosis. Lanes 1 and 6: H6PAK2H6 incubated with 40 μg of an inactive control lysate; lanes 2 and 7: 40 μg of active lysate with no exogenous H6PAK2H6 added; lanes 3 to 5: H6PAK2H6 incubated with 10, 20, and 40 μg of active rCPP32, respectively; lanes 8 to 11: 5, 10, 20, and 40 μg of active Jurkat lysate, respectively. CP, the COOH-terminal PAK2 cleavage product, detected by immunoblotting with COOH-terminal–directed anti-Ste20. (**B**) Recombinant His-tagged (H6) PAK1 or PAK2 were incubated with lysates from Fas-stimulated Jurkat cells, as described (*14*). Lanes 1 and 7: PAK1H6 and H6PAK2H6, respectively, incubated with 40 μg of inactive control lysate; lanes 2 and 8: 40 μg of active Jurkat lysate alone; lanes 3 to 6 and 9 to 12: PAK1H6 and H6PAK2H6 incubated with 5, 10, 20, and 40 μg of active Jurkat lysate, respectively. (**C**) Wild-type (WT) H6PAK2H6 and H6PAK2H6D212N protein were incubated either with inactive control lysate (control) or active recombinant CPP32 (rCPP32), as described (*15*). Active rCPP32 without H6PAK2H6 (–) served as a control. Similar resistance to cleavage of the PAK2 D212N mutant was observed in apoptotic cell lysates. The partial cleavage fragment seen just below the intact PAK2 WT and D212N proteins represents a non–caspase-related proteolysis product whose formation was not increased by CPP32.

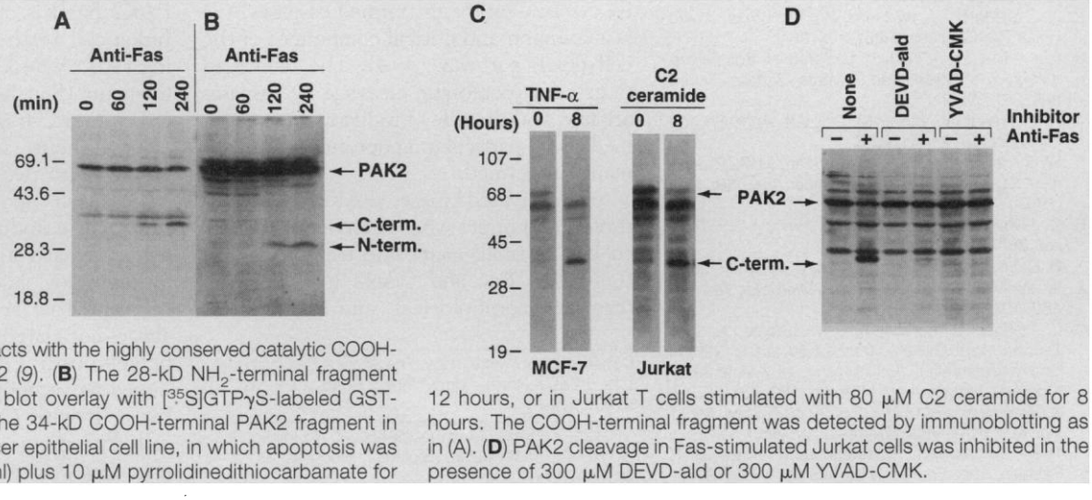

Fig. 1. Proteolytic cleavage of PAK2 in Fas-stimulated Jurkat T lymphocytes is blocked by ICE inhibitors. The formation of NH_2- and COOH-terminal cleavage products of PAK2 was measured at the indicated times after stimulation by Fas cross-linking. (**A**) Formation of the 34-kD COOH-terminal fragment (C-term.) was detected by immunoblotting with COOH-terminal–directed anti-Ste20, which cross-reacts with the highly conserved catalytic COOH-terminus of mammalian PAK2 (*9*). (**B**) The 28-kD NH_2-terminal fragment (N-term.) was detected by a blot overlay with [^{35}S]GTPγS-labeled GST-Rac1 (*11*). (**C**) Formation of the 34-kD COOH-terminal PAK2 fragment in either the MCF-7 breast cancer epithelial cell line, in which apoptosis was induced with TNF-α (20 ng/ml) plus 10 μM pyrrolidinedithiocarbamate for 12 hours, or in Jurkat T cells stimulated with 80 μM C2 ceramide for 8 hours. The COOH-terminal fragment was detected by immunoblotting as in (A). (**D**) PAK2 cleavage in Fas-stimulated Jurkat cells was inhibited in the presence of 300 μM DEVD-ald or 300 μM YVAD-CMK.

after Fas ligation (Fig. 3) with a time course that paralleled PAK2 cleavage (Fig. 1A). The in vitro–cleaved PAK2H6 protein had the same activity pattern in the in-gel kinase assay, and recombinant PAK2 catalytic domain (amino acids 213 to 525) was also active (Fig. 3). Little activation of the intact PAK2 protein was detected.

To investigate the role of PAK in the apoptotic program, we generated two independently derived Jurkat T cell lines (TD8 and TA12) stably expressing the PAK(H83L,H86L,K299R) dominant-negative mutant kinase (*22*) under an isopropyl-β-D-thiogalactopyranoside (IPTG)–inducible promoter (*23*). Expression of PAK(H83L,H86L,K299R) was induced about threefold and fivefold in the TD8 and TA12 cell lines, respectively, in the presence of IPTG, as determined by immunoblotting. Although Fas ligation still induced cell death in Jurkat cells expressing dominant-negative PAK(H83L,H86L,K299R), as indicated by DNA fragmentation, these apoptotic cells had abnormal morphological changes (*24*). Cells expressing dominant-negative PAK did not form apoptotic bodies during Fas-induced killing (>90% inhibition as compared to control Jurkat cells), but rather remained as intact rounded cells in which DNA fragmentation could still be detected by terminal deoxynucleotidyl transferase–mediated dUTP nick-end labeling (TUNEL) assay (Fig. 4A). One explanation for the inhibition of apoptotic body formation in TA12 cells could be that the onset of apoptosis is retarded in these cell lines. However, the normal kinetics of nuclear fragmentation and proteolytic cleavage of the CPP32 substrate D4 guanosine diphosphate dissociation inhibitor (*25*) do not support this hypothesis (*16*).

The process of phosphatidylserine (PS) export to the outer leaflet of the plasma membrane is an early and caspase-dependent event during apoptosis of cells from numerous lineages (*26*, *27*). When we examined the exposure of PS at the cell surface, as measured by the binding of annexin-V–fluorescein isothiocyanate (FITC) (*28*), we again found that the dominant-negative PAK had a pronounced effect. At early times, the induced TA12 cells, which express higher amounts of dominant-negative PAK, had nearly twice the annexin binding as did the noninduced and control cells (Fig. 4B). At later times, the "leaky" noninduced TA12 cells reached a level of annexin binding similar to that of the induced cells, which plateaued at a level about twice that of control Jurkat cells (Fig. 4B). Thus, blocking PAK function during Fas-induced apoptosis inhibited the morphological changes but accelerated the PS externalization in the membrane, whereas the nuclear modifications were unaffected.

We have identified a different mechanism through which PAK2 becomes activated—its proteolytic cleavage in response to activation of the caspase protease cascade by apoptotic stimuli. Because PAK2 is ubiquitously distributed in mammalian tissues, it is likely to play a role in caspase-mediated apoptotic events in a variety of systems. Our data suggest that the proteolytic release of intact PAK2 NH_2- and COOH-terminal fragments affects the actinomyosin system of the apoptotic cell. The caspase cascade has been termed the "executioner" of cell death (*3*): PAK2 appears to be one of its many swords.

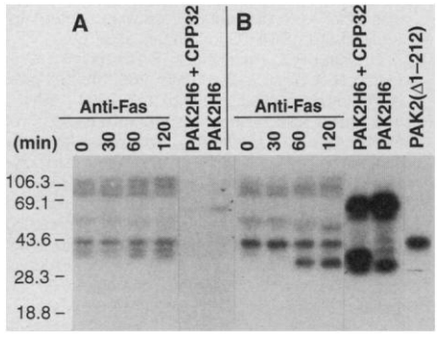

Fig. 3. Constitutive activation of PAK2 catalytic domain after CPP32-mediated proteolysis. The kinase activity of PAK2 was assessed by use of an in-gel kinase assay with p47*phox* peptide as the substrate (*20*, *21*). Autodioradiograph of the gel (**A**) without peptide substrate and (**B**) with peptide substrate incorporated. Recombinant purified PAK2H6 was also examined for kinase activity after treatment in the presence or absence of rCPP32, as indicated. Because of six histidines fused to the COOH-terminus of PAK2H6, the resulting CPP32 cleavage product migrates at a slightly higher molecular mass than the endogenous PAK2 cleavage product. The last lane contains recombinant PAK2 truncated at the NH_2-terminal (lacking amino acids 1 to 212) to generate the COOH-terminal fragment resulting from CPP32-mediated cleavage of intact PAK2. This construct was tagged with six histidines and the pET28 linker peptide at the NH_2-terminus and an additional six histidines at the COOH-terminus and consequently migrates at a substantially slower rate than the untagged cleavage product.

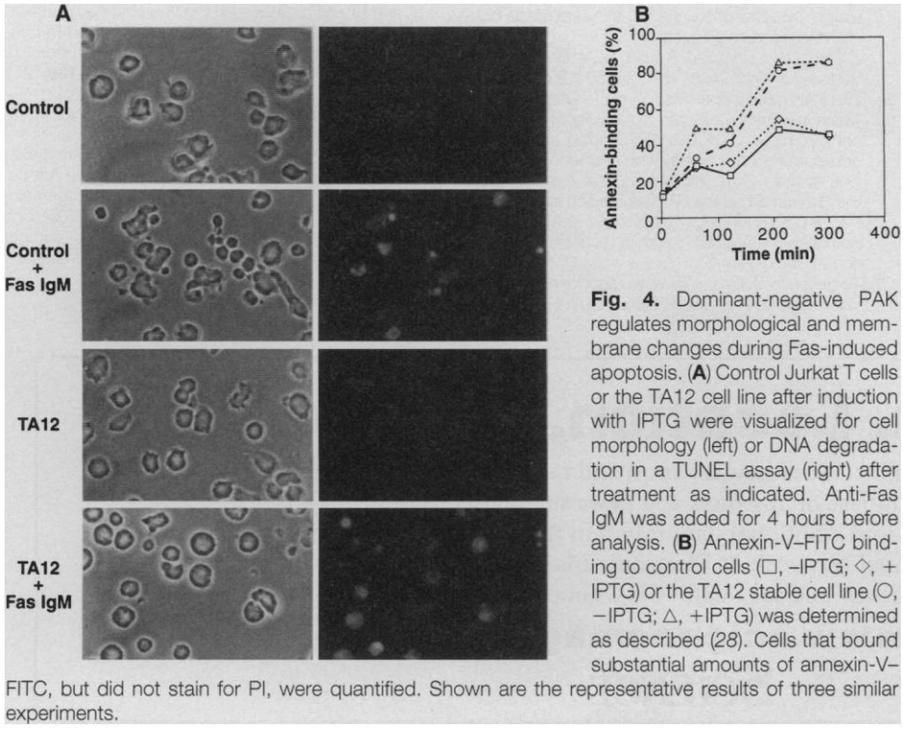

Fig. 4. Dominant-negative PAK regulates morphological and membrane changes during Fas-induced apoptosis. (**A**) Control Jurkat T cells or the TA12 cell line after induction with IPTG were visualized for cell morphology (left) or DNA degradation in a TUNEL assay (right) after treatment as indicated. Anti-Fas IgM was added for 4 hours before analysis. (**B**) Annexin-V–FITC binding to control cells (□, –IPTG; ◇, +IPTG) or the TA12 stable cell line (○, –IPTG; △, +IPTG) was determined as described (*28*). Cells that bound substantial amounts of annexin-V–FITC, but did not stain for PI, were quantified. Shown are the representative results of three similar experiments.

REFERENCES AND NOTES

1. S. J. Martin, D. R. Green, T. G. Cotter, *Trends Biochem. Sci.* **19**, 26 (1994); G. Majno and I. Joris, *Am. J. Pathol.* **246**, 3 (1995); M. K. T. Squier, A. J. Sehnert, J. J. Cohen, *J. Leukocyte Biol.* **57**, 2 (1995).
2. E. S. Alnemri *et al.*, *Cell* **87**, 171 (1996).
3. A. M. Chinnaiyan and V. M. Dixit, *Curr. Biol.* **5**, 555 (1996); S. J. Martin and D. R. Green, *Cell* **82**, 349 (1995); M. Whyte, *Trends Cell Biol.* **6**, 245 (1996); B. J. Yuan, *Curr. Opin. Cell Biol.* **7**, 211 (1995).
4. J. Schlegel *et al.*, *J. Biol. Chem.* **271**, 1841 (1996); M. Tewari *et al.*, *Cell* **81**, 801 (1995); K. Kuida *et al.*, *Nature* **384**, 368 (1996).
5. E. Manser, T. Leung, H. Salihuddin, Z. Zhao, L. Lim, *Nature* **367**, 40 (1994).
6. U. G. Knaus, S. Morris, H.-J. Dong, J. Chernoff, G. M. Bokoch, *Science* **269**, 221 (1995).
7. M. A. Sells *et al.*, *Curr. Biol.* **7**, 202 (1997).
8. H. Brzeska, U. G. Knaus, Z. Wang, G. M. Bokoch, E. D. Korn, *Proc. Natl. Acad. Sci. U.S.A.* **94**, 1092 (1997); C. Wu *et al.*, *J. Biol. Chem.* **271**, 31787

(1996); S. Dharmawardhane, R. H. Daniels, S. S. Martin, G. M. Bokoch, in preparation.
9. For detection of PAKs by immunoblots, the proteins were separated on 11% polyacrylamide gels and transferred to nitrocellulose filters (Millipore). The filters were blocked in Blotto (5% nonfat dry milk, 0.2% NP-40, 0.02 NaN_3) and incubated in anti-PAK1 or anti-PAK2 antisera (*6*) or NH_2-terminal–directed anti-Ste-20 VI (Kinetek Biotechnology, Vancouver, BC) diluted in 50 mM tris, 2 mM $CaCl_2$, 80 mM NaCl, 10% Blotto (pH 8). After extensive washes in 20 mM tris, 150 mM NaCl, 0.1% Tween-20 (pH 7.5), bound antibodies were visualized either by ^{125}I-PrA (Amersham) or by horseradish peroxidase–labeled secondary antibody in conjunction with enhanced chemiluminescence (Amersham) by exposing the filters to Kodak XOMAT film. In some cases, alkaline phosphatase–conjugated protein A and a color reaction mediated by bromochloroindolyl phosphate–nitro blue tetrazolium (BCIP-NBT) was used.
10. Apoptosis was induced by addition of anti-Fas IgM (150 ng/ml; Immunotech) to Jurkat T cells in complete medium for the times indicated. Jurkat T cells were suspended in propidium iodide buffer [0.1% Na citrate, 0.1% Triton X-100, propidium iodide (20 μg/ml)] and analyzed by fluorescence-activated cell sorting (FACS) as described (*29*).
11. A GTPase overlay assay was performed to detect the NH_2-terminal caspase cleavage product of PAK2. Briefly, cleared lysates of Jurkat T cells were separated on polyacrylamide gels and transferred to Trans-Blot nitrocellulose membranes (Bio-Rad), and filters were treated as described (*6*). The filters were incubated with purified Rac1 protein prelabeled with [^{35}S]GTPγS for 30 min at 4°C and for 10 min at room temperature. After several washes in phosphate-buffered saline (PBS), 5 mM $MgCl_2$, 0.05% Triton X-100, and 0.05% Tween 20, the filters were dried and exposed on Hyperfilm (Amersham).
12. Y. A. Lazebnik, S. H. Kaufmann, S. Desnoyers, G. G. Poirier, W. C. Earnshaw, *Nature* **371**, 346 (1994); N. A. Thornberry, H. G. Bull, J. R. Calayeay, K. T. Chapman, A. D. Howard, *ibid.* **356**, 768 (1992).
13. D. W. Nicholson *et al.*, *ibid.* **376**, 37 (1995).
14. To obtain active, nonrecombinant caspase fractions, we treated Jurkat T cells with anti-Fas IgM (150 ng/ml; Immunotech) for 3 to 4 hours. At this time point, more than 50% of the cells showed clear signs of apoptosis, such as DNA fragmentation, membrane blebbing, and apoptotic body formation. Cells were washed in ice-cold PBS and lysed in 25 mM Hepes, 0.1% CHAPS, 1 mM dithiothreitol (DTT), 0.5 mM phenylmethylsulfonyl fluoride, leupeptin (0.5 μg/ml), and aprotinin (10 μg/ml). Cleared lysates were used as active protease fractions in digests of PAK fusion proteins. In general, 300 ng of PAK fusion protein were incubated with 30 μg of either active Jurkat lysate or lysates of *E. coli* expressing recombinant CPP32 in a total volume of 30 μl of 25 mM Hepes, 1 mM DTT (pH 7.5) at 37°C for 1 hour.
15. For construction of the H6PAK2H6 and H6PAK2(213–525)H6 fusion proteins, either the complete *pak2*(1–1574) or the *pak2* fragment from position 636 to 1574 were amplified by polymerase chain reaction (PCR) with the distal primers GCGGATCCATGCTCGATAACGGAGAACT (TR201) and GCGGATCCATGGGTGCTGCCAAGTCTTTAGA (TR202), respectively, and the proximal primer CGCTCGAGACGGTTACTCTTCATTGCTT (TR203) for both reactions. Fragments that contained a PCR-engineered Bam HI site at the 5′ end and a Xho I site at the 3′ end were subcloned into the pET28a expression vector (Novagene). Mutation D212N was introduced in the pET28-*pak*2 by use of the Transformer Site-Directed mutagenesis kit (Clontech) and primer CAGTTGGTGATTCACATGTTAATGGTGCTGCCAAGTCTTTA (TR210). These constructs were transformed into *E. coli* strain BL21(DE3) pLysS for protein production. Cells grown to an absorbance at 590 nm of 0.6 in LB medium containing kanamycin (30 μg/ml) and chloramphenicol (30 μg/ml) were induced for 2 to 4 hours at 25°C in the presence of 0.5 mM IPTG. Histidine fusion proteins were purified on Ni^{2+}–nitrilotriacetic acid resin (Qiagen).
16. T. Rudel and G. M. Bokoch, data not shown.
17. Complementary DNA encoding CPP32 was cloned in-frame into the Bam HI–Eco RI site of pGEX-4T-3. Expression of CPP32 and preparation of active bacterial lysates has been described (*25*); expression was induced in exponentially growing bacteria by addition of 1 mM IPTG for 3 hours at 37°C.
18. P. R. Sleath, R. C. Hendrickson, S. R. Kronheim, C. J. March, R. A. Black, *J. Biol. Chem.* **265**, 14526 (1990); A. D. Howard *et al.*, *J. Immunol.* **147**, 2964 (1991).
19. The amino acid sequence surrounding Asp^{212} of PAK2 (Glu-Val-*Asp*-Gly-Ala) compares favorably with that of the known CPP32 cleavage site in poly-(ADP ribose) polymerase (His-Val-*Asp*-Gly-Ile).
20. For in-gel kinase assays, samples were resolved on standard 11% polyacrylamide gels containing p47*phox* peptide (amino acids 297 to 331) (0.5 mg/ml), which was shown to be a substrate for PAKs (*6, 21*). Gels were washed first in 20% 2-propanol, 50 mM tris (pH 7.5), then in 50 mM tris (pH 7.5), 5 mM β-mercaptoethanol before a denaturation step in 6 M guanidinium-HCl. For renaturation of proteins, gels were washed extensively in 50 mM tris (pH 7.5), 0.04% Tween-40, 5 mM β-mercaptoethanol and in PAK kinase buffer (PKB: 50 mM Hepes, 10 mM $MgCl_2$, 2 mM $MnCl_2$, 1 mM DTT). In-gel phosphorylation was done in PKB containing 10 μCi of [γ-^{32}P]ATP (adenosine 5′-triphosphate) per milliliter (5000 Ci/mmol) and 20 μM ATP for 30 min at 30°C. The gels were washed several times in 5% (w/v) trichloroacetic acid and 1% sodium pyrophosphate, stained with Coomassie blue, and dried for autoradiography.
21. J. Ding, U. G. Knaus, J. P. Lian, G. M. Bokoch, J. A. Badwey, *J. Biol. Chem.* **271**, 24869 (1996).
22. This PAK mutant contains a $Lys^{299} \rightarrow$ Arg mutation, which inactivates the catalytic activity of the kinase domain; mutation of this ATP binding site induces dominant-negative activity when introduced into various kinases (*30*). The presence of the His^{83} and His^{86} mutations in the GTPase binding site prevents Rac or Cdc42 binding (*7*), which allowed us to avoid potentially complicating effects resulting from titration of Rac or Cdc42.
23. To generate stable cell lines, we subcloned the dominant-negative PAK1(H83L,H86L,K299R) into the Not I site of the pOPI3 chloramphenicol acetyltransferase (CAT) vector (Stratagene), which allows IPTG-inducible expression in the presence of the Lac repressor. Before transfection, pOPI3-CAT PAK1(H83L,H86L, K299R) was linearized with Dra III and purified. Ten micrograms of the purified fragment were added to 1×10^7 Jurkat T cells, which were already stably transfected with the lacI-encoding p3′SS vector (Stratagene), and electroporated. Transfected cells were cultivated for 24 hours before addition of G418 (1 mg/ml; Gibco-BRL) to select for transfectant clones. To ensure the clonal origin, transfectants were aliquoted in serial dilutions into 96-well culture plates and expanded only from plates with less than 10 G418-resistant clones per 96-well plate.
24. To compare the morphological changes of Jurkat T cells and the TA12 mutant line during apoptosis, we performed a TUNEL assay using the ApopTag Plus In Situ Apoptosis Detection Kit (Oncor, Gaithersburg, MD). Anti-Fas IgM (150 ng/ml) or C2 ceramide (80 μM) were added to the cells for 4 hours or 18 hours, respectively, in normal medium at 37°C and 5% CO_2. The cells were washed in PBS, fixed in 3.8% formaldehyde, and air-dried on microscope slides. Nicked and degraded DNA was labeled by use of the terminal deoxynucleotidyl transferase (TdT) reaction with digoxygenin-labeled nucleotides and fluorescein-conjugated anti-digoxygenin. The samples were mounted with Fluoromount-G (Southern Biotechnology Associates, Birmingham, AL) and viewed under a Nikon Labophot-2 microscope at 100× magnification.
25. S. Na *et al.*, *J. Biol. Chem.* **271**, 11209 (1996).
26. S. J. Martin *et al.*, *J. Exp. Med.* **182**, 1 (1995); I. Vermes, C. Haanen, H. Steffens-Nakken, C. Reutelingsperger, *J. Immunol. Methods* **184**, 39 (1995); G. Koopman *et al.*, *Blood* **84**, 1415 (1994).
27. S. J. Martin, D. M. Finucane, G. Amarante-Mendes, G. A. O'Brien, D. R. Green, *J. Biol. Chem.* **271**, 28753 (1996); D. M. Vanags, M. I. Pörn-Ares, S. Coppola, D. H. Burgess, S. Orrenius, *ibid.*, p. 31075.
28. Exposure of PS was quantified by annexin-V–FITC binding and flow cytometry with the Apoptosis Detection Kit (R&D Systems). Jurkat T cells and mutant cell line TA12 were incubated with anti-Fas IgM for the indicated time, washed with PBS, and resuspended in binding buffer. Annexin-V–FITC and PI were added, and the samples were analyzed by flow cytometry in a FACScan (Becton Dickinson). Annexin-V–FITC was measured in the FL1 channel, and PI was measured in the FL3 channel. Annexin-V–FITC binding positive-staining cells and PI negative-staining cells were scored as apoptotic.
29. I. Nicoletti *et al.*, *J. Immunol. Methods* **139**, 271 (1991).
30. S. K. Hanks, A. M. Quinn, T. Hunter, *Science* **241**, 42 (1988).
31. We thank T.-H. Chuang for assistance with Jurkat transfection procedures and for scientific advice. Supported by the Deutsche Forschungsgemeinschaft (T.R.) and NIH grants HL48008 and GM39434 (G.M.B.). This is publication number 10589-IMM from The Scripps Research Institute.

10 March 1997; accepted 13 May 1997